12th International Congress on the Deterioration and Conservation of Stone
Columbia University, New York, 2012

MIRABILITE AND HEPTAHYDRATE CHARACTERIZATION FROM INFRARED MICROSCOPY AND THERMAL DATA.

Mélanie Denecker [(1)], Ronan Hébert [(1)], Ann Bourgès [(2)], Beatriz Menendez [(1)], and Eric Doehne [(3)]

[(1)] Géosciences et Environnement Cergy, Université de Cergy-Pontoise, F-95031 Cergy-Pontoise cedex. Contact author: melanie.denecker@u-cergy.fr
[(2)] Laboratoire de Recherche des Monuments Historiques (LRMH), 29 rue de Paris, 77420 Champs sur Marne, France
[(3)] Conservation Sciences, Pasadena, CA, USA

Abstract

Sodium sulfate is widely regarded as the most damaging salt for porous building materials. To understand this complex and incompletely understood phenomena, it is important to predict which phases will crystallize under a range of environmental conditions and which phase transitions will cause damage. In this study we present data on the crystallization of sodium sulfate hydrates from infrared spectroscopy and temperature data.
This work documents the crystalline phases and their transitions under controlled environmental conditions (temperature and relative humidity, RH). The phase changes in a salt crystal coming from a droplet of sodium sulfate solution (28 and 30 wt. % of Na_2SO_4) subjected to evaporation are observed using FTIR-ATR spectroscopy. As Na_2SO_4 hydrates contain more OH content than anhydrous phase, the OH absorption band enables the distinction between these two types of phases. The temperature signal are acquired using a type K thermocouple in a solution of sodium sulfate (28 and 30 wt.% of Na_2SO_4) that is cooled down from +40 °C to +5 °C. As the temperature decreases, crystallization events are recorded though the temperature signal. According to temperature monitoring experiments, heptahydrate crystallizes more easily than mirabilite.
The importance of the environmental conditions and the protocol establishment are discussed. The approach of these methods can help us to understand the crystallization sequence of sodium sulfates and later better apprehend the damage of building stone.

Keywords: Sodium sulfate, crystallization, FTIR-ATR spectroscopy, thermocouple

1. Introduction

Sodium sulfate attack is one of the most damaging decay phenomena for building stones. The main damage results from the cyclic crystallization of salts in pores (Goudie and Viles, 1997), especially hydrates which crystallize rapidly at a high supersaturation (Rodriguez- Navarro et al., 2000; Tsui et al., 2003; Steiger and Asmussen, 2003; Flatt, 2002). The study of sodium sulfate crystallization ultimately aims at preventing salt

deterioration of important building materials in order to improve the conservation of cultural heritage and also any kind of construction.

Sodium sulfates occur as several phases: the decahydrate (mirabilite, $Na_2SO_4 - 10\ H_2O$) and the anhydrous (thenardite, Na_2SO_4) phases crystallize under normal ambient conditions (figure 1). A second hydrate (heptahydrate, $Na_2SO_4 - 7\ H_2O$) was noted in the middle of the 19th (Loewel, 1850) and is metastable. Several studies (Loewel, 1850; De Coppet, 1901; Hartley et al., 1908) showed that heptahydrate crystallizes first during cooling of a bulk solution, rather than mirabilite. The heptahydrate can be obtained either by cooling a sodium sulfate solution (Hamilton and Hall, 2008; Derluyn et al., 2011) or a material whose pores are saturated with a sodium sulfate solution (Rijniers et al., 2005; Hamilton and Hall, 2008; Hamilton et al., 2008; Espinosa-Marzal and Scherer, 2008).

In the present study we perform temperature cycles on sodium sulfate solutions under confined conditions in order to crystallize the hydrates of sodium sulfate. During these cycles we record the temperature of the solution in order to observe exo and/or endothermic reac- tions that are linked to important phase transitions. We also use Fourier Transform Infrared Attenuated Total Reflection (FTIR-ATR) in order to investigate the crystallization changes from droplets of sodium sulfate solution during evaporation.

In the following section, the experimental approaches by FTIR-ATR and temperature monitoring are described. Then the experimental results for each method are discussed and the importance of environmental conditions and testing protocols are emphasized.

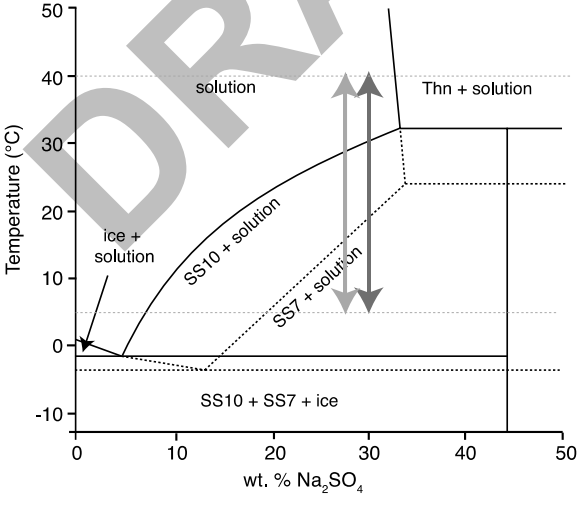

Figure 1: Na_2SO_4-H_2O phase diagram (after Negi and Anand, 1985; with the solubility data tabulated in Garrett, 2001; Brand, 2009) at room pressure showing stable (solid lines) and metastable (dashed lines) phase boundaries. The different domains such as thenardite (thn), mirabilite (SS10) and heptahydrate (SS7) are represented. The solutions, with 28 and 30 wt. % of Na_2SO_4 (respectively light gray and dark gray lines), are cooled down from +40 to +5 °C through the mirabilite and heptahydrate solubility lines

2. Experimental approaches

2.1 Material

Na_2SO_4 solutions with a concentration of 28 and 30 wt. % of Na_2SO_4 are prepared using anhydrous Na_2SO_4 (Natriumsulfat ROTH, ≥ 99.0 %) dissolved in demineralized water at +60 °C. Droplets of about ~ 100 µl are used in the case of FTIR-ATR spectroscopy, whilst we used volumes of 30 ml of solution for the temperature monitoring.

2.2 FTIR-ATR spectroscopy

FTIR-ATR spectra were measured using a Perkin-Elmer, Spectrum 100 FTIR-ATR. Spectra were acquired in the wavenumber interval of 530-4000 cm−1 with a spectral resolution of 4 cm−1. Each spectrum was recorded from the accumulation of 10 scans of a sample set on the ATR crystal. All measurements were made at 55 ± 3 % of relative humidity (RH) corresponding to the room RH.
The aim of this measurement consists to investigate the evolution of the crystal formed from a droplet of Na_2SO_4 solution at room temperature (T = 20 ± 0.5 °C) under evaporation condition. A solution droplet, initially at 60 °C, is placed on the ATR platinum which is at room temperature (figure 2). The spectra are recorded immediately as soon as the crystallization of the first salt crystal takes place and after different time of evaporation step.
An infrared spectrum gives a fingerprint of a sample with absorption bands. Each absorption band corresponds to the frequencies of vibration between the chemical bonds of a specific atom making up the material. Each material has a specific combination of atoms which produce a typical infrared spectrum.

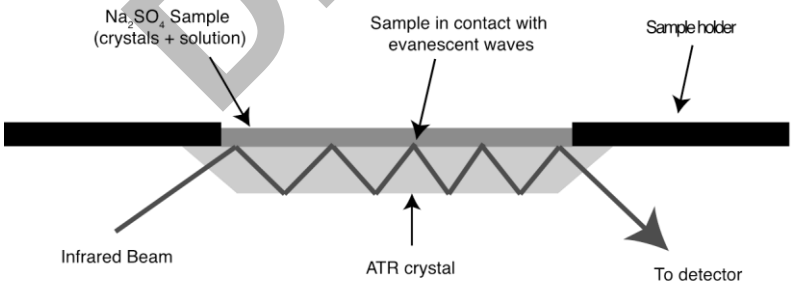

Figure 2: Protocol device used for FTIR-ATR spectroscopy. Droplet of Na_2SO_4 solution is put directly on the ATR crystal.

2.3 Thermal monitoring

A serie of 3 temperature cycles was performed using a climatic test chamber Binder

MKF with a program control (figure 3). The temperature range of the climatic chamber is -40 °C up to +180 °C with an accuracy of ±1.0 °C, and the RH range is between 10 % and 98 % RH with a precision of ± 2.0 % RH. The RH was neglected as the experiment was performed under confined conditions.

The test is composed of cooling/heating cycles based on previous works that were proven to be efficient to crystallize heptahydrate (Hamilton and Hall, 2008; Derluyn et al., 2011). It starts at +40 °C with an cooling phase down to +5 °C, where the temperature, very close to the heptahydrate supersolubility line, is maintened during 10 hours. The cooling phase aims to crystallize the heptahydrate. A rate of 0.33 °C.min−1 was used for the cooling as well as for the heating. The temperature of the samples was measured with a precision of ± 0.1 °C, via a type K thermocouple that was dipping into the solution at the bottom of the bottle. The temperature was recorded every 5 seconds using a data logger (Agilent).

Basic analysis was performed on the temperature signal of the climatic chamber (reference) and the solution samples. A frequency filtering was applied in order to remove the noise probably related to the periodic activity of the climatic chamber.

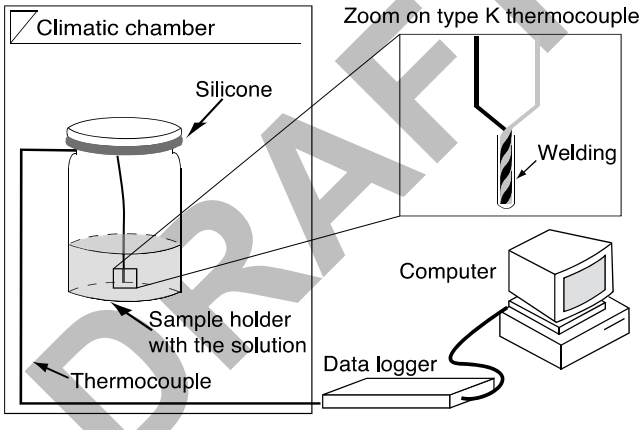

Figure 3: Experimental set-up for the temperature monitoring: samples are placed in a climatic chamber (Binder) where they undergo cooling/heating cycles. The temperature is recorded via a type K thermocouple that dips into the solution. A silicon sealant joint is dispatched around the cap of the bottle in order to obtain the best confinement of the sodium sulfate solutions.

3. Results and Discussion

3.1 Crystallization from Na_2SO_4 droplets

Figures 4a and 4b present FTIR-ATR spectra of sodium sulfate crystals coming from a droplet of solution at room temperature after different times of evaporation. Each spectrum corresponds to an average spectrum from the accumulation of multiple spectra sampled in a given surface. The response is characteristic to each component of the sample studied. The absorption in the regions 1575-1700 cm−1 and 3650-3100 cm−1 show the presence of ν-OH bonds(Weiss 1969), respectively ν1-OH and ν2-OH, which correspond to two different modes of vibration between -OH bonds. Those at 580-670

cm−1 (Weiss 1969) and 1000-1300 cm−1 (Durie and Milne 1978; Tong et al 2010) correspond to the part of $-SO_4^{2-}$bonds, respectively ν1-SO_4^{2-} and ν2-SO_4^{2-}. The band size in the spectrum can be considered as a direct indication of the amount of material present.

Figure 4a shows FTIR-ATR spectra of crystal from a droplet of solution with 28 wt.% of Na_2SO_4. It indicates a decreasing of the ν1-OH and ν2-OH bands intensity from t=0 to t=3h30 with a band shift from 3350 to 3422 cm^{-1} for ν2-OH. This decreasing in bands intensity consists to a decreasing of OH content. The intensity of the ν1-SO_4^{2-} band develops strongly after t=1h30. The ν2-SO_4^{2-} band remains the same during all the experiment. Figure 4b presents FTIR-ATR spectra of crystal from a droplet of solution with 30 wt. % of Na_2SO_4. It shows an increasing of the ν1-OH, ν2-OH and ν2-SO_4^{2-} bands intensity from t=0 to t=2h corresponding to an increasing of OH and $-SO_4^{2-}$ contents. After t=2h, the ν-OH bands intensity highly decreases and the ν2-OH band moves from 3345 to 3400 cm^{-1} whilst the ν-SO_4^{2-} bands remain constant (i.e. the ν2-SO_4^{2-} band) and/or intensifies (i.e. the ν1-SO_4^{2-} band) as it has been observed in figure 4a.

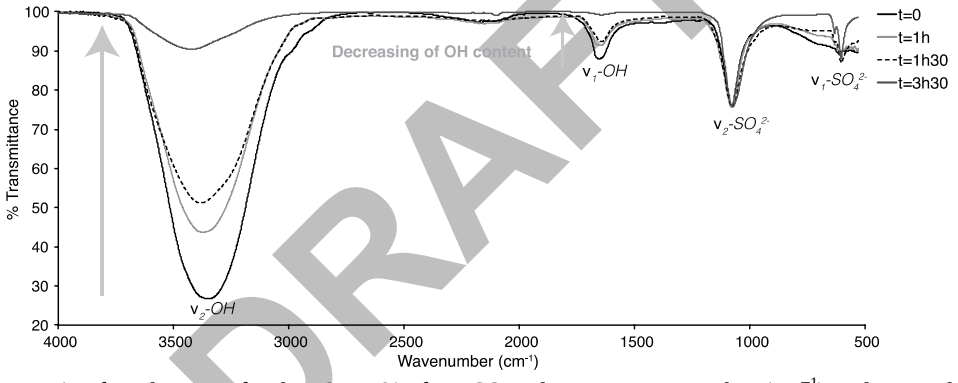

a) Infrared spectra for the 28 wt. % of Na_2SO_4 solution vs wavenumber (cm^{-1}) under T and RH constant

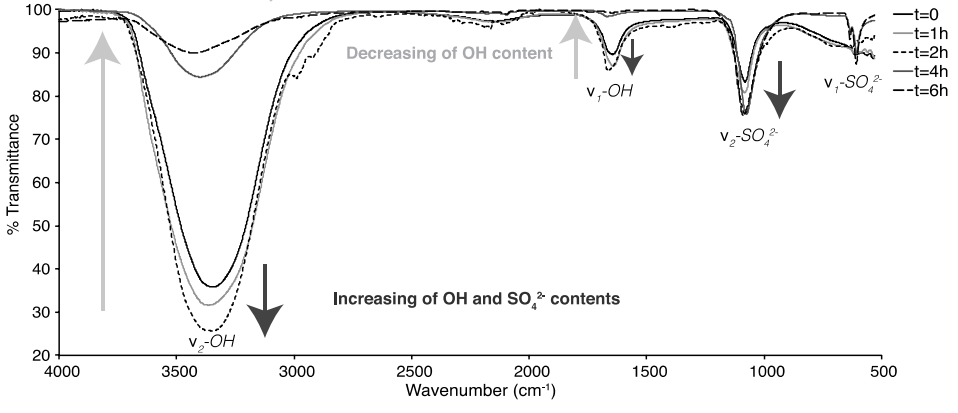

(b) Infrared spectra for the 30 wt. % of Na_2SO_4 solution vs wavenumber (cm^{-1}) under T and RH constant

Figure 4: Infrared spectra are made on crystals forming in the Na_2SO_4 droplet at room temperature (T=20 °C ± 0.5 °C) and room RH (55 % ± 2 %). The t=0 curve is the occurence of the first crystal. The crystal remains at room temperature and RH during the all experiment.

3.2 Crystallization from Na_2SO_4 solutions

In figure 5, the temperature signal of the climatic chamber (i.e. temperature reference, black curve) and the solution samples of two different concentrations (i.e. 28 and 30 wt. % of Na_2SO_4, respectively green and red curves) are represented.
During the first cycle, the temperature signal of the solution with 28 wt. % of Na_2SO_4 follows that of the reference during the cooling from +40 °C to the plateau at +5 °C where a temperature peak is observed. It forms a smooth and asymmetrical peak starting at ~5.56 °C. This peak occurs over a large period of time (~ 155.45 min) and has a low height (peak maximum ~0.69 °C). It is characterized by a progressive and slow temperature increase. Once the exothermic peak is over, the temperature signal of the solution joins that of the reference. During the heating stage to back at +40 °C, we can observe a slight shift of the temperature signal of the solution starting at ~17.35 °C until the end of the cycle. The second cycle presents similar results except that the exothermic peak starting at ~5.77 °C seems to be lower. Indeed, this peak occurs on a shorter period of time (~137.14 min) and has a lower height (peak maximum ~0.44 °C) than the previous cycle. A slight shift of the solution temperature starting at ~20.59 °C is observed when heating back to +40 °C. An additional third cycle reveals the disappearance of the exothermic reaction close to the plateau at +5 °C. The cooling of the solution is strongly slowed down near to ~ 7.85 °C causing a shift between the temperature signal of the reference and that of the solution. Once again during the heating stage, the temperature of the solution is slightly shifted compared with the temperature signal of the reference starting at ~ 18.38 °C.

The temperature signal of the solution with 30 wt. % of Na_2SO_4 presents some differences compared to the precedent temperature signal. The first cycle shows a smooth asymmetrical peak of temperature starting at ~ 6.94 °C as it has been observed previously. This peak of temperature occurs on a large time period equal to ~ 114.54 min with a low height (peak maximum ~0.75 °C). The second and third cycles do no present peak of temperature during the cooling period. As it has been observed for the third cycle of the previous temperature signal of the 28 wt. % of Na_2SO_4 solution, the cooling of the solution with 30 wt. % of Na_2SO_4 is strongly slowed down close to ~9.5 °C causing a shift between the temperature signal of the reference and that of the solution. During the heating stage of each cycle, we can observe the same results as seen previously.

3.3 Discussion

FTIR-ATR and temperature monitoring were used to investigate the crystallization

changes in a sodium sulfate solution under confined condition undergoing cooling/heating cycles and in droplets of solution subject to evaporation. FTIR-ATR enables to follow the evolution of crystals that form from a 28 wt % of a Na_2SO_4 solution. It shows a general decreasing of the ν-OH bands intensity that can be due to a decrease of the OH content in the crystal. The ν- SO_4^{2-} bands remain constant (i.e. the ν2- SO_4^{2-} band) and/or increase (i.e. the ν1- SO_4^{2-} band). This change can be due to the dehydration process: the hydrate transforms progressively into anhydrous Na_2SO_4

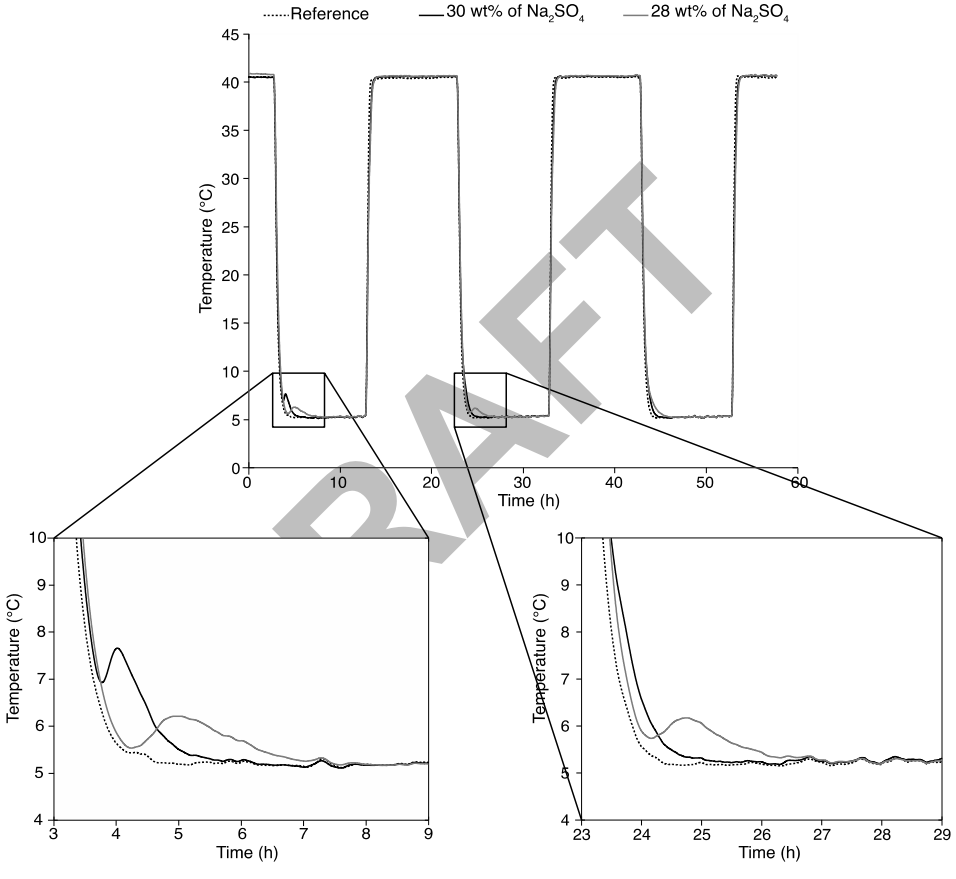

Figure 5: Temperature vs time diagram for temperature monitoring: temperature signals of the climatic chamber (reference, black curve), the 28 wt% of Na_2SO_4 (green curve) and the 30 wt% of Na_2SO_4 (red curve) solutions during 3 successive cooling/heating cycles. Zooms on the two first cooling phase close to +5 °C are represented

during evaporation. The evolution of crystal from a droplet of solution with 30 wt. % of Na_2SO_4 can be divided in two parts. In the first part, the intensity of the ν-OH and ν2- SO_4^{2-} bands increase from t=0 to t=2h. This increase can be linked to the crystal growth

process. The second part may result from the dehydration process occuring during the crystallization of the anhydrous phase as previously described. As we can see in figures 4a and 4b, the duration of these experiments is too short to completely achieve the anhydrous Na_2SO_4 (OH bands still present). This suggests a possible mixing problem between the crystal and the surrounding solution. It would be necessary to isolate the crystal in order to have no effect of the solution (i.e. to work on monocrystal) and use for example a confinement cell to maintain the temperature and the relative humidity.

The temperature signal of the solutions (i.e. with 28 and 30 wt. % of Na_2SO_4) does not show a good reproducibility from a cycle to another. Indeed, only one exothermic peak on the temperature signal of the solution with 30 wt. % of Na_2SO_4 is observed. In the first and second cycle, the temperature signal of the solution with 28 wt. % of Na_2SO_4 presents an exothermic peak, which decreases in intensity until no peak is distinguishable (i.e. cycle 3). The exothermic peaks occur progressively and are not instantaneous as it is the case for the crystallization of mirabilite according to Rodriguez-Navarro and Doehne (1999). Moreover, their description, which is consistent with published data of Hamilton et al. (2008), Derluyn et al. (2011), and Saidov (2012) indicates that these peaks of temperature correspond to the crystallization of the metastable heptahydrate. One hypothesis for the non reproducibility from a cycle to another is that the system is not completely reset at the end of a cycle, i.e. that the duration of the plateau at +40 °C is not long enough to allow the complete dissolution of the crystals present in the solution. Thus, when cooling again, there is no nucleation process to take place but just crystal growth which requires less energy. One way to investigate this hypothesis would be to increase the duration of the step at +40 °C or increase the temperature target in order to favor the dissolution of all the remaining crystals in the solution.

4. Conclusion

FTIR-ATR spectroscopy is a innovative experience to charaterize the transformations during the crystallization process such as the crystal growth and/or the dehydratation of salt crystals coming from droplets subjected to evaporation conditions. The preliminary results on the two different concentrations of the solutions (i.e. 28 and 30 wt. % of Na_2SO_4) present a progressive transformation of Na_2SO_4 hydrate into anhydrous phase. The temperature monitoring confirms that the crystallization of heptahydrate occurs easily close to +5 °C upon cooling a solution saturated.

5. Acknowledgment

Mélanie Denecker is indebted to the Cergy-Pontoise University for financial support and the Laboratoire de Recherche des Monuments Historiques (LRMH) for access to analytical facili- ties. This research is supported by the Fondation des Sciences du Patrimoine.

6. References

Brand, H. (2009). Thermoelastic properties of salt hydrates and implication for geological structures. University College London. Thesis. 240

De Coppet, L.C. (1901). Sur l'heptahydrate de sulfate de sodium. Bull. Soc. Vaud. Sci. Nat. XXXVII 141, 455-462.

Derluyn, H., Saidov, T. A., Espinosa-Marzal, R. M., Pel, L., & Scherer, G. W. (2011). Sodium sulfate heptahydrate I: The growth of single crystals. *Journal of Crystal Growth*, *329*(1), 44-51.

Durie, R.A., Milne, J.W. (1978). Infrared spectra anhydrous alkali métal sulphates. Spectrochimica Acta, 34A, 215-220.

Espinosa Marzal, R. M., & Scherer, G. W. (2008). Crystallization of sodium sulfate salts in limestone. *Environmental Geology*, *56*(3-4), 605-621.

Flatt, R. J., & Scherer, G. W. (2002). Hydration and crystallization pressure of sodium sulfate: a critical review. *Materials Research Society Symposium Proceedings*, *712*(Materials Issues in Art and Archaeology VI), 30, 2001, Boston, Ma.

Garrett, D. E. (2001): *Sodium sulfate: handbook of deposits, processing, properties, and use*. Academic Press.

Goudie, A., Viles, H. (1997). Salt Weathering Hazards. Wiley, Chichester

Hamilton, A., & Hall, C. (2008). Sodium sulfate heptahydrate: a synchrotron energy-dispersive diffraction study of an elusive metastable hydrated salt. *Journal Of Analytical Atomic Spectrometry*, *23*(6), 840-844.

Hamilton, A., Hall, C., & Pel, L. (2008). Sodium sulfate heptahydrate: direct observation of crystallization in a porous material. *Journal of Physics D: Applied Physics*, *41*(21), 212002.

Hartley, H., Jones, B. M., Hutchinson, G. A., & Jones, G. (1908). The Spontaneous Crystallization of Sodium Sulfate Solutions. *Journal of the Chemical Society Transactions*, *433*(7021), 825-833.

Loewel, H. (1850). Observations sur la sursaturation des dissolutions salines. *Ann. Chim. Phys.*, *29*, 62–127.

Max, J.-J., & Chapados, C. (2001). IR spectroscopy of aqueous alkali halide solutions: Pure salt-solvated water spectra and hydration numbers. *The Journal of Chemical Physics*, *115*(6), 2664.

Negi, A. S., & S. C. Anand (1985): *A textbook of physical chemistry*. New Age Publishers. Orlando, T. M., T. B. McCord, & G. A. Grieves (2005): The chemical nature of Europa's surface material and the relation to a subsurface ocean. *Icarus* 177(2), 528-533

Rijniers, L. A., Huinink, H. P., Pel, L., & Kopinga, K. (2005). Experimental evidence of crystallization pressure inside porous media. *Physical Review Letters*, *94*(7), 075503.

Rodriguez-Navarro, C., & Doehne, E. (1999). Salt weathering: influence of evaporation rate, supersaturation and crystallization pattern. *Earth Surface Processes and Landforms*, *24*(3), 191-209. John Wiley & Sons.

Rodriguez-navarro, C., Doehne, E., & Sebastian, E. (2000). How does sodium sulfate crystallize ? Implications for the decay and testing of building materials. *Cement and Concrete Research*, *30*(10), 1527-1534.

Steiger, M., & Asmussen, S. (2008). Crystallization of sodium sulfate phases in porous materials: The phase diagram Na2SO4-H2O and the generation of stress. *Geochimica et Cosmochimica Acta*, *72*(17), 4291-4306.

Tong, H.-J., Reid, J. P., Dong, J.-L., & Zhang, Y.-H. (2010). Observation of the crystallization and supersaturation of mixed component NaNO3-Na2SO4 droplets by FTIR-ATR and Raman spectroscopy. *The Journal of Physical Chemistry A*, *114*(46), 12237-12243.

Tsui, N., Flatt, R. J., & Scherer, G. W. (2003). Crystallization damage by sodium sulfate. (T. Takanami & G. Kitagawa, Eds.)*Journal of Cultural Heritage*, *4*(2), 109-115.

Weiss, P. (1969). Infrared spectroscopy. Its use in the coatings Industry. Infrared Spectroscopy Committee of the Chicago Society for Paint Technology, Federation of Societies for Paint Technology, Philadelphia, 1969. X + 456 pp. 20.00 to members, 30.00 to nonmembers. *Journal of Applied Polymer Science*, *13*(11), 2509-2509.